A compositional method to model dependent failure behavior based on PoF models

Zhiguo Zeng, Yunxia Chen, Enrico Zio, Rui Kang

Chinese Journal of Aeronautics 28 (2016) xx-xx **Final Accepted Version**

Contents lists available at ScienceDirect

Chinese Journal of Aeronautics

journal homepage: www.elsevier.com/locate/cja

A compositional method to model dependent failure behaviors based on PoF models

Abstract

In this paper, a new method is developed to model dependent failure behaviors among failure mechanisms. Unlike existing methods, the developed method models the root cause of the dependency explicitly, so that a deterministic model, rather than a probabilistic one, can be established. Three steps comprise the developed method. First, physics-of-failure (PoF) models are utilized to model each failure mechanism. Then, interactions among failure mechanisms are modeled as a combination of three basic relations, competition, superposition and coupling. This is the reason why the method is referred to as "compositional method". Finally, the PoF models and the interaction model are combined to develop a deterministic model of the dependent failure behaviors. As a demonstration, the method is applied on an actual spool and the developed failure behavior model is validated by a wear test. The result demonstrates that the compositional method is an effective way to model dependent failure behaviors.

Keywords: Dependent failures, physics-of-failure, reliability modeling, multiple dependent competing failure processes, degradation, shock

1. Introduction

Physics-of-failure (PoF) methods are widely applied to model components' failure behaviors. In most PoF methods (e.g., [1]), failure mechanisms are modeled first by deterministic PoF models [2-4], and, then, by assuming that all the failure mechanisms are independent, the PoF model with the shortest time to failure (TTF) is used to describe the failure behavior of a component [1]. A fundamental assumption in PoF methods is that all the failure mechanisms are independent. This assumption, however, does not hold in many real cases, because in practice, failure mechanisms are often dependent [5]. For example, it is observed from experimental data that two failure mechanisms, like erosion and corrosion, can enhance each other, resulting in faster degradation [6]. Another example is that when test specimens are susceptible to high temperatures and heavy loads, fatigue can interacts with creep so that the specimens' TTFs are severely reduced [7].

In the literature, many effective methods have been developed to model such dependent failure behaviors, e.g., the multivariate distribution method (see, for example, [8] and [9]), the copula-based method (see, for example, [10]), and the shock-degradation interaction method (see, for example, [11] and [12]). In the multivariate distribution method, the dependency is modeled by identifying the joint probability distribution of the dependent variables and estimating the distribution parameters based on failure data. For example, if two components of a series system are dependent, the reliability of the system is

$$R(t) = P_{T_1,T_2}\left(T_1 > t, T_2 > t\right),$$

where T_1, T_2 denote the TTFs of the two components and $P_{T_1,T_2}(\cdot)$ is their joint distributions. In [13], $P_{T_1,T_2}(\cdot)$ was assumed to be a Marshall-Olkin bivariate Weibull distribution and the parameters of the distribution were estimated from failure data.

References [14] and [15] reviewed the commonly used multivariate TTF distributions. Kotz et al. [8] investigated how the efficiency of parallel redundancy was affected when the two components were positively or negatively quadrant dependent. Navarro et al. [16-18] used the concept of Samaniego's signature to obtain the mean time to failure and bounds for the reliability of dependent coherent systems. Cui and Li [19] developed an approach based on a Markov process to determine the joint TTF distribution of coherent systems with dependent components. Lai and Lin [9] extended the result in [8] by deriving new formulas to calculate the two-sided bounds of the MTTF of a parallel system with two dependent components.

The multivariate distribution method is a simple and straightforward method to model dependent failure behaviors. However, the method is based on probabilistic models and requires large amount of failure data to estimate the parameters of the models, which limits its applicability.

A copula of the random vector $[Z_1, Z_2]$ is defined as the joint cumulative distribution function of $[U_1, U_2]$,

$$C(u_1, u_2) = P[U_1 \le u_1, U_2 \le u_2],$$

where U_1 and U_2 are defined by $(U_1, U_2) = \left(F_1(Z_1), F_2(Z_2)\right)$, in which $F_i(\cdot)$ is the cumulative distribution function of Z_{i} [20]. According to Sklar's Theorem, the joint distribution function of any random vector can be expressed as the marginal distribution of each element and a copula that describes the dependency [20]. Thus, the joint probability distribution can be determined by estimating the marginal distributions and the copula separately.

Bunea and Bedford [21] developed a model where the dependency among competing risks is modeled by a copula. A similar model was developed in [22, 23], as well as a discussion on how the choice of copulas affected the estimated reliability. Yang et al. [24] used copulas to investigate the reliability of a partially perfect repairable system. Hong et al. [25] illustrated optimal condition-based maintenance in systems, whose dependency is described by copulas. In [26] and [27], copulas were applied to model the failure behavior of a microgrid and a static network, respectively. Wang et al. [10] introduced a time-varying copula-based method to model the dependency between degradation processes and random shocks. In [28], Jeddi et al. discussed the redundancy allocation problem when the components' lifetimes are dependent and described by copulas. Zhang et al. [29] used copulas to develop statistical inference methods for systems subject to dependent competing failures. Wu [30] established a new asymmetric copula and applied it to fit two-dimensional warranty data. Ebrahimi and Li [31] used copulas to account for the dependency among atoms and calculated the reliability of a nanocomponent.

As the multivariate distribution method, the copula-based method is also based on probabilistic models and relies on failure data to estimate the model parameters. The only difference is that, in the multivariate distribution method, we identify the joint probability distribution directly, whereas in the copula-based method, we only have to identify the marginal probability distributions and the copula and the joint probability distribution is calculated using Sklar's Theorem [20]. Thus, the copula-based method shares the same limitation as the multivariate distribution method, that is, large amount of failure data need be collected to estimate the model parameters.

Another important dependency model is the shock-degradation interaction model developed by Feng and Coit [11]. In this model, two dependent failure processes, a degradation process and a shock process, are considered. Both processes can lead to failures and the degradation process is influenced by the shocks. The failure processes are referred to as multiple dependent competing failure processes (MDCFPs). Feng and Coit [11] assumed the arriving shock would bring an abrupt increase to the normal degradation process and developed a probabilistic model to calculate the system's reliability. Wang and Pham [32] used a similar approach as [11] to model the DCFPs and determined the optimal imperfect preventive maintenance policy. Peng et al. [12] applied the model in [11] to calculate the reliability of a micro-engine and determined the optimal maintenance strategy. Keedy and Feng [33] applied the model in [11] on a stent, where the degradation process was modeled by a PoF model. Song et al. considered the reliability of a system whose components were subject to the MDCFPs [34] and distinct component shock sets [35]. Apart from the model in [11], the MDCFPs can be modelled in many other ways. Jiang et al. [36] extended the work in [11] by assuming that the threshold of the degradation process was shifted by shocks. Rafiee et al. [37] developed a model in which the degradation rates were modified by different shock patterns. Fan et al. [38] developed a Stochastic Hybrid System (SHS) based framework for reliability modeling and analysis of MDCFPs. Zhang et al. [39] considered epistemic uncertainty in MDCFP modeling using a Probability Box (P-box) based approach.

The shock-degradation interaction method provides new insights into dependency modeling by considering the actual way in which the dependency arises. However, this method only deals with a simplified scenario, where dependency arises from the superposition of two independently evolving failure mechanisms. By "independently evolving", we mean that the failure behavior of each failure mechanism is not changed by the other failure mechanism. In practice, however, rather than evolving independently, the failure mechanisms might be actually coupled. Examples of coupling include the interaction between erosion and corrosion [6], and between fatigue and creep [7]. The effect of coupling should thus be considered, when modeling multiple dependent failure mechanisms.

As reviewed before, most these existing methods are grounded on probabilistic models. Therefore, they share a common limitation: the requirement on large amount of data for the accurate estimation of model parameters. To address this problem, we develop a mechanistic approach in this paper, which explicitly models the root cause of dependency to develop a deterministic model, rather than a probabilistic one, to describe the dependent failure behaviors. The rest of this paper is organized as follows. In Section 2, we review the PoF-based failure behavior modeling method using the concept of performance parameters. The compositional method is developed in Section 3 and applied in Section 4 to model the dependent failure behavior of a spool. Experimental validation of the developed model is also conducted in Section 4. Finally, in Section 5, the paper is concluded with a discussion on potential future works.

2. Performance parameters and PoF models

In this paper, failure behaviors are described by performance parameters and modeled based on PoF models. In this section, we first introduce the two concepts and then, discuss how to use the two concepts to describe failure behaviors.

2.1. Performance parameters and failure behaviors

Failure is defined as the event or state for which a system or component no longer fulfills its intended function [2-4]. In most cases, failures can be described by performance parameters and failure thresholds.

Definition 1 (Performance parameters and failure thresholds). Suppose the required function of a system (or component) is not fulfilled if and only if the following inequality holds,

$$p \geq p_{th}. \tag{1}$$

Then, parameter p is defined as the performance parameter, while p_{th} is defined as the failure threshold associated with performance parameter p.

From Definition 1, a failure state is reached whenever a performance parameter exceeds its associated failure threshold. In other words, the smaller the value of the performance parameter is, the safer the system (or component) will be. This kind of performance parameters are referred to as smaller-the-better (STB) parameters. In reality, there are also larger-the-better (LTB) and nominal-the-best (NTB) parameters, whose definitions can be generalized easily from Definition 1. For simplicity of illustration, we assume that all the performance parameters discussed in this paper are STB.

Example 1. The designed function of a beam is to withstand a given load. Thus, the performance parameter of the beam is its stress, σ, which results from the applied load. The failure threshold p_{th} is the strength of the beam, $[\sigma]$. Whenever $\sigma \geq [\sigma]$, the beam fails.

Example 2. The designed function of a spool is to control hydraulic oil flows. When the oil leaks, the spool no longer fulfills its function. Thus, leakage is defined as the failure state of the spool. Increases of clearances due to wear will cause the leakage. Therefore, the clearance, denoted by x, is the performance parameter of the spool. The failure threshold, x_{th}, is the clearance when the leakage takes place. Whenever $x \geq x_{th}$, the spool fails.

Definition 2 (Failure behaviors). Failure behaviors of a system (or component) are defined as the observable changes of the system's (or component's) states during its failure process.

Since p and p_{th} in Definition 1 can be used to characterize failures, the failure behavior can be described by modeling the variation of p over time, as shown in Figure 1.

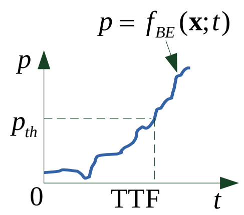

Figure 1 Describing failure behaviors by modeling the variation of p over time

In Figure 1, $f_{BE}(\cdot)$ represents the failure behavior model (FBM), in which $\mathbf{x}$ is a vector of input parameters. By substituting p_{th} into the FBM and solving for t, the TTF of the system (or the component) can be determined.

2.2. Using PoF models to describe failure behaviors

The variation of p in Figure 1 is caused by failure mechanisms. Failure mechanisms are the physical or chemical processes which lead to failures [40]. In this section, we discuss how to model the failure mechanisms based on PoF models. These failure mechanism models are, then, combined to model the failure behavior of the component, considering the interactions among them, which will be discussed in detail in Sect. 3.

Definition 3 (PoF models). If the physics behind the failure mechanisms is well understood, physics-based models can be built to predict the behavior of the failure-inducing processes. These physics-based models are referred to as physics-of-failure models (PoF models).

Research on PoF models dates back to the late nineteenth century when A. Wohler investigated the effect of fatigue on railway axles [41]. Since then, common failure mechanisms have been intensively investigated and many effective PoF models have been developed. For a review of PoF models commonly used in electronic and mechanical products, readers might refer to [2-4]. PoF models can be used to determine the values of the performance parameters, which are used to describe the failure behavior of the system (or component), as shown in Figure 1.

Example 3. According to Example 2, the performance parameter of the spool is its clearance, denoted by x. Since the spool is subject to adhesive wear, the Archard model in (2) is often used as its PoF model [42].

$$\frac{dx_{adh}}{dt} = K_{adh}\frac{W_a}{H_m} = k_1. \tag{2}$$

In (2), x_{adh} is the wear depth caused by adhesive wear, K_{adh} is a constant associated with surface conditions and lubrication, W_a is the normal load on the wear surfaces, H_m is the hardness of the wear surface and k_1 is the wear rate.

The performance parameter x can be derived based on (2), since $x = x_0 + x_{adh}$, where x_0 is the initial clearance. Substituting the previous expression into (2), the failure behavior of the valve can be described.

PoF models like (2) describe the failure-inducing process. However, a variety of PoF models only provide information about the TTF. For example, the Coffin-Manson model is a commonly applied model to describe low-cycle fatigue [4]:

$$\mathrm{TTF}=\left(\Delta\epsilon_P \big/ 2\epsilon_f^{'}\right)^{1/C}, \tag{3}$$

where $\Delta\epsilon_p/2$ is the plastic strain amplitude, $\epsilon_f^{'}$ is the fatigue ductility coefficient and C is the fatigue ductility exponent.

In order to use PoF models like (3) to describe failure behaviors, we need to define a dummy variable $D, D \ge 0$, which represents the damage caused by the failure mechanism and stipulate that a failure occurs whenever $D \ge 1$. We can easily verify from Definition 1 that D is a performance parameter and its associated failure threshold is $D_{th} = 1$. Thus, the failure behavior can be described by D.

To derive D from the PoF models, assumptions on how the damage accumulates need to be made. Often, Miner's rule of linear accumulation is used [4], so that

$$\begin{aligned} D &= kt, \\ k &= \frac{1}{\mathrm{TTF}}. \end{aligned} \tag{4}$$

where TTF is determined by the PoF models. Equation (4) is used to describe the failure behavior of the system (or the component) based on PoF models like (3), which only predicts the TTF. It should be noted that the damage accumulation model in Eq. (4) is based on a strict assumption of linear accumulation. In practice, more complex situations might exist which requires more advanced damage accumulation models.

Example 4. In this example, we use the damage, D, to describe the failure behavior resulted from low-cycle fatigue, based on the Coffin-Manson model in (5). The failure threshold associated with D is $D_{th} = 1$. By using Miner's rule in (4), the failure behavior can be described by

$$D = \left(\Delta\epsilon_P \big/ 2\epsilon_f^{'}\right)^{-1/C} \cdot t, \tag{5}$$

where $\Delta\epsilon_P, \epsilon_f^{'}$ and C have the same meaning as in (3).

3. The compositional method to model dependent failure behaviors

In this section, we investigate the interactions among failure mechanisms and develop a compositional method to model the dependent failure behaviors. The method is called "compositional" because it assumes that the interactions among failure mechanisms can be modeled as a combination of three basic relations: competition, superposition and coupling. The interactions among failure mechanisms are modeled first in Sect. 3.1; then, in Sect. 3.2, the dependent failure behavior is modeled by combing the PoF models considering the interactions among them.

3.1. Modeling of the interactions

In this section, we develop a method to model the interactions as a combination of three basic relations. The three basic relations, competition, superposition and coupling, are introduced first in sections 3.1.1-3.1.3. Then, in Sect. 3.1.4, a visualization tool, the interaction graph, is developed, to model the interactions in terms of the three basic relations.

3.1.1 Competition

Competition refers to the situation where each failure mechanism contributes to a specific performance parameter and the presence of one failure mechanism has no influence on the others, as shown in Figure 2.

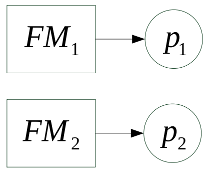

Figure 2 Illustration of competition

In Figure 2, FM_i and p_i refer to the i th failure mechanism and its performance parameter, respectively.

Example 5. An example of competition is the interaction among the three failure mechanisms of a composite ply [43]. There are three failure mechanisms for the composite ply, fiber tensile, matrix failure and fiber kinking/ splitting. According to [43], the composite ply can fail due to either of the three failure mechanisms. Moreover, the three failure mechanisms have no influence on one another. Thus, competition applies to the three failure mechanisms.

3.1.2 Superposition

Superposition refers to the situation where all the mechanisms contribute to a common performance parameter and the presence of one failure mechanism has no influence on the others, as shown in Figure 3. In Figure 3, FM_1 and FM_2 denote the failure mechanisms, p_1 denotes the common performance parameter, while $p_{FM,1}, p_{FM,2}$ represent the contribution of the corresponding failure mechanism, respectively.

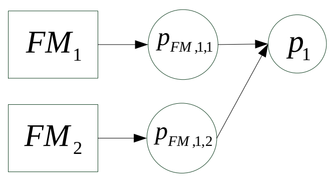

Figure 3 Illustration of superposition

Example 6. An example of superposition is the interaction between the pitting and corrosion-fatigue suffered by structures [44]. Let a denote the crack size. The structure fails whenever a exceeds the maximum allowable crack size, a_{th}. Thus, a is the performance parameter of the structure. According to [44], both pitting and corrosion-fatigue lead to the growth of the crack and thus, contribute to the degradation of the common performance parameter a. Therefore, superposition applies to the two failure mechanisms.

3.1.3 Coupling

Coupling refers to the situation where the presence of one mechanism influences the other failure mechanisms. Coupling is caused by the synergistic effect among the coupled failure mechanisms, in which one failure mechanism changes the inputs of the other failure mechanisms, as described in Figure 4.

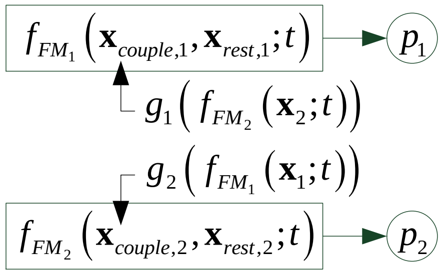

Figure 4 Illustration of coupling

In Figure 4, two failure mechanisms, FM_1 and FM_2 are coupled. The $f_{FM,1}(\cdot)$ and $f_{FM,2}(\cdot)$ are the PoF models for the coupled failure mechanisms, while p_1 and p_2 are corresponding performance parameters. Some of the inputs to the $f_{FM,1}(\cdot)$ and $f_{FM,2}(\cdot)$, denoted by $\boldsymbol{x}_{couple,1}$ and $\boldsymbol{x}_{couple,2}$, are influenced by the other failure mechanism and thus result in coupling between the two failure mechanisms. These parameters are referred to as coupling factors. The influence from the other failure mechanism is represented by $g_1(\cdot)$ and $g_2(\cdot)$.

Example 7. An example of coupling is the interaction between fatigue and creep [7]. According to [7], when specimens are subject to these two failure mechanisms, the resistance to fatigue is reduced due to the influence of creep. Thus, the two failure mechanisms are coupled.

Example 8. Another example of coupling can be found in specimens subject to erosion and corrosion [6]. According to [6], erosion removes the protection layer on the specimen, which makes the specimen more prone to corrosion and results in an increased corrosion rate [6].

3.1.4 The interaction graph

The first step of the compositional method is to model the interactions among failure mechanisms. In this paper, it is assumed that the interactions are composed of the three basic relations. A visualization tool, the interaction graph, is developed in this section to visualize how the interactions are composed in terms of the three basic relations.

In an interaction graph, a box represents a failure mechanism while a circle denotes a performance parameter. An arrow from a box to a circle means that the performance parameter corresponding to the circle is influenced by the failure mechanism corresponding to the box. A diamond is a symbol for coupling. If coupling exists between two failure mechanisms, a diamond is placed between the corresponding boxes, with the coupling factors written inside the diamond. An illustration of the interaction graph is given in Figure 5.

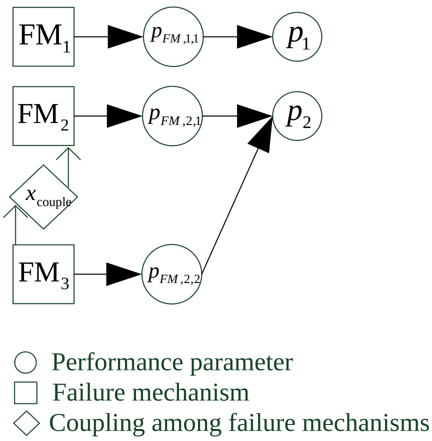

Figure 5 A illustration of interaction graph

Once the interaction graph is constructed, we can easily determine how the interactions are composed. For example, for the interaction graph in Figure 5, it can be seen from the Figure that superposition and coupling exist between failure mechanisms 2 and 3, while competition exists among failure mechanisms 1, 2, and 3. With the help of the interaction graph, the interaction among failure mechanisms is modeled as a combination of the three basic relations.

3.2. Modeling of the dependent failure behavior

In this section, we develop a method to model the dependent failure behavior. The failure behavior of a system (or a component) is influenced by the PoF models and the interactions among them. The interactions, as discussed in Sect. 3.1, are composed of the three basic relations. Thus, in Sect. 3.2.1 - Sect. 3.2.3, we first discuss how to model the influence of each basic relation. Then, in Sect. 3.2.4, a method is developed to model the failure behavior resulting from a combination of the basic relations.

3.2.1 Case 1: Only competition exists

Since the competing failure mechanisms contribute to different performance parameters and do not influence one another, the failure behavior can be modeled by the weakest-link model, whereby the failure mechanism with shortest TTF determines the failure behavior of the component (or system):

$$\mathrm{TTF}_{comp} = \min_{i=1}^{n} \mathrm{TTF}_{FM,i}. \tag{6}$$

In (6), TTF_{comp} means the TTF of the component (or system), n is the number of the failure mechanisms that the component (or system) is subject to and $\mathrm{TTF}_{FM,i}$ refers to the TTF predicted by the PoF model of the ith failure mechanism.

In some PoF models, the performance parameters do not change over time. For these models, equation (6) can be expressed in turns of the performance parameters. To do so, let us first define the performance margin of the ith failure mechanism, M_i, as

$$M_i = \frac{p_{th,i} - p_i}{p_{th,i}}, \tag{7}$$

where p_i and $p_{th,i}$ are the performance parameter and the failure threshold for the ith failure mechanism, respectively. It is obvious that a failure occurs whenever $M_i < 0$. Then, the weakest-link model can be expressed using the concept of performance margin:

$$M_{comp}=\min_{i=1}^{n}\left(M_i\right)=\min_{i=1}^{n}\left(\frac{p_{th,i}-p_i}{p_{th,i}}\right). \tag{8}$$

In (8), M_{comp} stands for the performance margin of the component (or system). The component (or system) fails whenever $M_{comp}<0$. Equation (8) states that the failure mechanism with the least performance margin determines the failure behavior of the component (or system). Suppose the jth failure mechanism has the minimum performance margin, that is, $M_{comp}=M_j$. Then, the performance parameter of the component is determined by the performance parameter of the jth failure mechanism, $p_{comp}=p_j$. It is obvious that (6) and (8) are equivalent expressions of the weakest-link model.

Example 9. In this example, we use the proposed method to develop the failure behavior model for the composite ply in Example 5. According to [43], the PoF models for the failure mechanisms in Example 5 are given in (9)-(11).

$$p_1=\left(\frac{\sigma_1(t)}{\sigma_L^+(t)}\right)^2, p_{th,1}=1, \tag{9}$$

where σ_1 is the main stress and σ_L^+ is the tensile strength in the longitudinal direction parallel to the fibers.

$$p_2=\left(\frac{\tau_{23}^{\phi_0}(t)}{\tau_T(t)-\mu_T\sigma_n^{\phi_0}(t)}+\frac{\tau_{12}^{\phi_0}(t)}{\tau_L(t)-\mu_L\sigma_n^{\phi_0}(t)}+\frac{\sigma_{n+}^{\phi_0}(t)}{\sigma_T^+(t)}\right), p_{th,2}=1, \tag{10}$$

where $\tau_{23}^{\phi_0},\tau_{12}^{\phi_0},\sigma_n^{\phi_0}$ are the components of stresses in the specific directions, τ_T,τ_L,σ_T^+ are the corresponding strengths and μ_L,μ_T are friction coefficients in the specific directions.

$$p_3=p_{split}=\left(\frac{\tau_{23}^{m_0}(t)}{\tau_T(t)-\mu_T\sigma_2^{m_0}(t)}\right)^2+\left(\frac{\tau_{12}^{m_0}(t)}{\tau_T(t)-\mu_T\sigma_2^{m_0}(t)}\right)^2+\left(\frac{\sigma_{2+}^{m_0}(t)}{\sigma_T^+(t)}\right), p_{th,3}=1, \tag{11}$$

where the meaning of each parameter is consistent with those in (9) and (10).

Since competition applies to the three failure mechanisms of the ply, the weakest link model in (8) is used to model the interactions among failure mechanisms. Since $p_{th,1}=p_{th,2}=p_{th,3}=1$, equation (8) can be simplified:

$$p=\max\left(p_1,p_2,p_3\right), p_{th}=1. \tag{12}$$

In (12), p and p_{th} refer to the performance parameter and failure threshold of the composite ply under the joint effect of the three failure mechanisms. The p_1,p_2,p_3 are determined from (9)-(11), respectively. The results in (12) are the same as those obtained in [43].

3.2.2 Case 2: Only superposition exists

Superposition of failure mechanisms can be modeled by summing up the contribution from each failure mechanism. Suppose that superposition applies to n_i failure mechanisms, where the jointly contributed performance parameter is denoted by $p_i, 1\le i\le n$. Then, the superposition can be modeled as:

$$p_i=\sum_{j=1}^{n_i}p_{FM,i,j}=\sum_{j=1}^{n_i}f_{FM,i,j}\left(\boldsymbol{x}_{ij},t\right). \tag{13}$$

In (13), $p_{FM,i,j}$ is the contribution of the jth failure mechanism and is determined by the corresponding PoF model, $f_{FM,i,j}\left(\boldsymbol{x}_{ij},t\right)$. When all the $f_{FM,i,j}\left(\boldsymbol{x}_{ij},t\right)$'s are derivable, (13) can be rewritten in the form of rate-summation:

$$\frac{dp_i}{dt}=\sum_{j=1}^{n_i}\frac{dp_{FM,i,j}}{dt}. \tag{14}$$

Example 10. In this example, we use (13) to model the superposition between two failure mechanisms in electronic devices. Both the two failure mechanisms contribute to the time-dependent dielectric breakdown (TDDB) [3]. Here, we assume that the two failure mechanisms do not influence each other. Thus, superposition is applied to model the interaction among them. The PoF models for the failure mechanisms are the E-model, given below in (15), and the 1/E model, given in (16):

$$\mathrm{TTF}_E = A_0 \exp\{-\gamma E_{ox}\} \exp\left\{\frac{Q}{K_B T}\right\}. \tag{15}$$

$$\mathrm{TTF}_{1/E} = \tau_0(T) \exp\left\{\frac{G(T)}{E_{ox}}\right\}. \tag{16}$$

In (15), γ is the field-acceleration parameter, E_{ox} is the electric field in the oxide, Q is the activation energy, A_0 is a process/material-dependent coefficient, K_B is the Boltzmann constant and T is the temperature in Kelvin. In (16), $\tau_0(T)$ and $G(T)$ are temperature-related constants.

In order to use (15) and (16) to describe the failure behavior of the component, we first define two dummy variables, D_E and $D_{1/E}$, to represent the damage caused by the corresponding failure mechanisms. Applying Miner's rule of damage accumulation in (4), we have

$$D_E = \frac{1}{\mathrm{TTF}_E} t,\ D_{1/E} = \frac{1}{\mathrm{TTF}_{1/E}} t, \tag{17}$$

where TTF_E and $\mathrm{TTF}_{1/E}$ are determined from (15) and (16), respectively.

Since superposition applies to the two failure mechanisms, from (14), we have

$$D = D_E + D_{1/E}. \tag{18}$$

In (18), D means damage of the component and is the performance parameter of the component.

Since $D > 1$ indicates a failure, by substituting (17) into (18), we have

$$\mathrm{TTF} = \frac{\mathrm{TTF}_E \cdot \mathrm{TTF}_{1/E}}{\mathrm{TTF}_E + \mathrm{TTF}_{1/E}}. \tag{19}$$

Equation (19) describes the failure behavior resulting from the superposition of E-model and 1/E-model. The result in (19) is the same as that obtained in [3].

3.2.3 Case 3: Only coupling exists

Coupling can be modeled by introducing the concept of coupling factors. It can be seen from Figure 4 that coupling is caused when some input parameters (the $\boldsymbol{x}_{couple,1}$ and $\boldsymbol{x}_{couple,2}$ in Figure 4) are changed by other failure mechanisms. These parameters are referred to as coupling factors.

In order to model the effect of coupling, the coupling factors need to be identified first. Then, the influence on the coupling factors from other failure mechanisms, (the $g_1(\cdot)$ and $g_2(\cdot)$ in Figure 4), is determined based on an analysis of the nature of the influence. Finally, by substituting the $g_1(\cdot)$ and $g_2(\cdot)$ into the corresponding PoF model, the effect of coupling can be modeled:

$$\begin{cases} p_1 = f_{FM_1}\left(\boldsymbol{x}_{rest,1}, \boldsymbol{x}_{couple,1}; t\right), \\ \boldsymbol{x}_{couple,1} = g_1\left(f_{FM_2}\left(\boldsymbol{x}_2; t\right)\right). \end{cases}$$
$$\begin{cases} p_2 = f_{FM_2}\left(\boldsymbol{x}_{rest,2}, \boldsymbol{x}_{couple,2}; t\right), \\ \boldsymbol{x}_{couple,2} = g_2\left(f_{FM_1}\left(\boldsymbol{x}_1; t\right)\right). \end{cases} \tag{20}$$

Example 11. In this example, we illustrate the method in (20) by modeling the coupling between fatigue and creep. For components subject only to low-cycle fatigue, a Coffin-Manson model is often used to approximate the failure behavior, as shown in (3) and (4). Since coupling exists between fatigue and creep, the k in (4) is assumed to be influenced by creep and is regarded as the coupling factor. In [4], it is assumed that k is influenced by creep as:

$$k = \frac{1}{\mathrm{TTF}} \cdot \upsilon^{-(k-1)} = \left(\Delta\epsilon_P / 2\epsilon_f^{'}\right)^{-1/C} \cdot \upsilon^{-(k-1)}, \tag{21}$$

where $\upsilon^{-(k-1)}$ describes the influence from creep. According to (20), by substituting (21) into (4), the performance parameter and TTF under the effect of coupling between fatigue and creep can be obtained:

$$D = kt = \left(\Delta\epsilon_P \Big/ 2\epsilon_f^{'} \right)^{-1/C} \cdot \upsilon^{-(k-1)} t,$$
$$\text{TTF} = \arg_t \left(D(t) = 1 \right) = \left(\Delta\epsilon_P \Big/ 2\epsilon_f^{'} \right)^{1/C} \cdot \upsilon^{(k-1)}. \tag{22}$$

It is easy to verify that the result in (22) is equivalent to the widely used frequency-modified Coffin-Manson model [4, 45]. It should be noted that an important feature of coupling is that, when coupling exists, the PoF models for the failure mechanisms are usually changed due to the effect of the coupled mechanisms. For example, in Example 11, due to the coupling effect from creep, the PoF model for fatigue (Eq. (22)) is different from the original Coffin-Manson model. This fact makes coupling distinct from superposition and competition, where in the latter two cases, the PoF models for each individual failure mechanism remains unchanged. Rather, the dependent failure behavior is caused by the joint effect of the PoF models. For example, in Example 10, although superposition exists between E-model and 1/E-model, the PoF model of each mechanism remains unchanged (Eq. (15) and (16)).

3.2.4 Case 4: Mixture of the three basic relations

In actual cases, the interaction among the failure mechanisms is a combination of the three basic relations. Thus, the modeling methods in Sect. 3.2.1-3.2.3 should be combined to model the actual dependent failure behavior. Suppose a general interaction graph in Figure 7 contains n performance parameters, which are denoted by $p_i, i = 1, 2, \cdots n$. Further, let us assume that the i th performance parameter is influenced by n_i failure mechanisms under superposition. Suppose the corresponding PoF models are

$$p_{FM,i,j} = f_{FM,i,j}\left(\boldsymbol{x}_{i,j}, t \right), \ j = 1, 2, \cdots, n_i. \tag{23}$$

where $p_{FM,i,j}$ is the performance parameter associated with the j th failure mechanism and $f_{FM,i,j}(\cdot)$ is the PoF model. Note that if the k th performance parameter p_k is subject to only one failure mechanism, then $n_k = 1$.

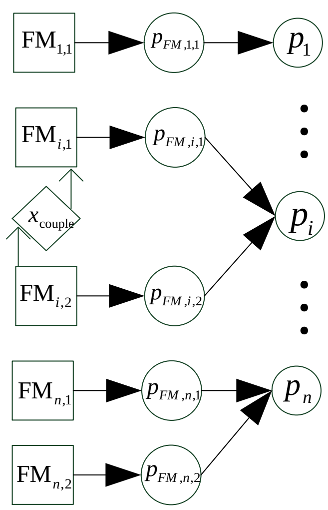

Figure 6 A general interaction graph

The dependent failure behavior can be modeled in two steps:

- First, determine the performance parameters according to (24):

$$p_i = \sum_{j=1}^{n_i} p_{i,j}, \tag{24}$$

where $p_{i,j}$ is the contribution of the j th failure mechanism on p_i and is determined by

$$p_{i,j} = \begin{cases} (23), & \text{if } FM_j \text{ is not subjected to coupling,} \\ (20), & \text{if } FM_j \text{ is subjected to coupling.} \end{cases} \tag{25}$$

- Next, since competition applies to all p_i s, the failure behavior of the system (or the component) can be predicted using (6) and (8).

Example 12. In this example, we use the compositional method to model the dependent failure behavior of the multiple dependent competing failure processes (MDCFPs) from [12]. In the MDCFP, a component is subject to the joint effect of three failure mechanisms [12].

The first failure mechanism, denoted by FM_1, is the overstress failure, which is caused by shocks. When a shock arrives, a damage of W will be incurred. If $W \geq D$, where D stands for the resistance to shocks, an overstress failure will happen. According to Definition 1, W is a performance parameter, and we denote it by p_1. The second failure mechanism, denoted by FM_2, results in gradual degradations of the performance parameter, p_2. When $p_2 > H$, a soft failure will be caused. Meanwhile, p_2 is also subject to the influence from the third failure mechanism, denoted by FM_3, which is caused by shocks: when the i th shock arrives, an additional degradation to p_2 will be caused.

In order to apply the compositional method, we first construct the interaction graph to visualize the interactions among the three failure mechanisms. The interaction graph is given in Figure 7.

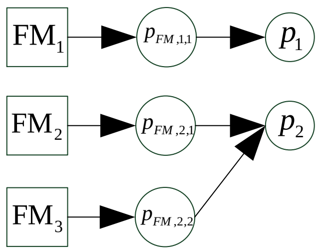

Figure 7 The interaction graph of the MDCFP

It can be seen from Figure 7 that p_2 is subject to the joint effect of FM_2 and FM_3, and the two failure mechanisms do not influence each other. Thus, superposition applies to FM_2 and FM_3. Also, since no interactions exist among FM_1, FM_2 and FM_3, competition applies to p_1 and p_2. According to (24) and (25), the p_1 and p_2 are determined by

$$\begin{aligned} p_1 &= p_{FM,1,1} = f_{FM_1}\left(\boldsymbol{x}_1;t\right), \\ p_2 &= p_{FM,2,1} + p_{FM,2,2} = f_{FM_2}\left(\boldsymbol{x}_2;t\right) + f_{FM_3}\left(\boldsymbol{x}_3;t\right), \end{aligned} \tag{26}$$

where, $f_{FM_i}\left(\boldsymbol{x}_i;t\right)$ is the PoF model for the i th failure mechanism.

Then, according to (6), the TTF is predicted by

$$\mathrm{TTF} = \min\left\{\mathrm{TTF}_1, \mathrm{TTF}_2\right\}. \tag{27}$$

In (27), TTF_1 and TTF_2 are determined by

$$\mathrm{TTF}_1 = \arg_t\left\{p_1(t) = p_{th,1}\right\}, \mathrm{TTF}_2 = \arg_t\left\{p_2(t) = p_{th,2}\right\}. \tag{28}$$

Equations (26)-(28) describe the failure behavior of the MDCFP. Further, we can use (26)-(28) to predict the reliability:

$$\begin{aligned} R(t) &= P\left(p_1(t) < p_{th,1}, p_2(t) < p_{th,2}\right) \\ &= P\left(p_1(t) < p_{th,1}\right) \cdot P\left(p_2(t) < p_{th,2}\right) \\ &= P\left(f_{FM_1}\left(\boldsymbol{x}_1;t\right) < p_{th,1}\right) \cdot P\left(f_{FM_2}\left(\boldsymbol{x}_2;t\right) + f_{FM_3}\left(\boldsymbol{x}_3;t\right) < p_{th,2}\right). \end{aligned} \tag{29}$$

When the arrival of shocks follows a Poisson process with rate λ, it is easy to verify that the result in (29) is equivalent to the one from [12]. Thus, this example demonstrates that the compositional method is effective in modeling a mixture of competition and superposition. In Sect.4, we will demonstrate, through an actual case study, that the method is also effective in modeling coupling.

It should be noted that a premise of applying the compositional method is that the interactions among the failure mechanisms are can be identified explicitly using the three basic relations defined in the paper. However, we admit that in some practical applications, especially when the interaction among the failures are complex, the interaction cannot be easily identified explicitly and, therefore, the compositional method cannot be applied. In this case, since the root cause of the dependency cannot be understood, we have to resort to probabilistic methods or design experiments and fit the failure behavior model from the collected data.

4. A case study

In this section, we use the compositional method to model the dependent failure behavior of an actual spool. We also design and implement a wear test, which validates the failure behavior model originated from the compositional method.

4.1. Failure mechanisms and PoF models

As discussed in Example 1, the performance parameter of the spool is its clearance, x. According to the result of a failure mode, mechanism, effect analysis (FMMEA) [46], since the spool and its sleeve are made from the same material, the spool is subject to adhesive wear. Besides, due to the possible existence of hard pollutants, the spool is also subject to three-body abrasive wear (hereafter referred to as abrasive wear) [46]. Adhesive wear can be modeled by Archard model [42], as shown in (2). Abrasive wear can be modeled by the following differential equation [47]:

$$\frac{dx_{abr}}{dt} = K_{abr}\frac{W_a}{H_m} = k_2. \tag{30}$$

In (30), K_{abr} is a constant associated with the properties of the wear surfaces, while the other parameters in (30) share the same meanings as those in (2). In actual cases, the values of k_1 and k_2 are often estimated from wear tests.

4.2. Modeling of the interactions

The interaction graph of the two failure mechanisms are given in Figure 8.

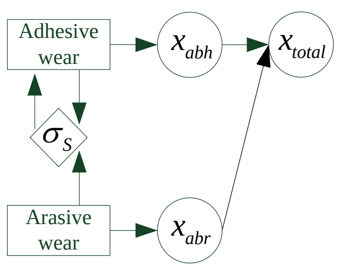

Figure 8 The interaction graph of the spool

From Figure 8, we can see that superposition exists between adhesive wear and abrasive wear, since both the two failure mechanisms contribute to a common performance parameter, the total wear depth, x_{total}. Besides, coupling between the adhesive wear and abrasive wear also exists.

From (24), the rate of x_{total} can be determined as

$$\frac{dx_{total}}{dt} = \frac{dx_{adh}}{dt} + \frac{dx_{abr}}{dt} = k_1 + k_2, \tag{31}$$

where k_1, k_2 are rate constants in (2) and (30), respectively.

The k_1 and k_2 in (31) are influenced by the coupling of adhesive wear and abrasive wear. From (2), k_1 is dependent on K_{adh}. According to [46], the K_{adh} is influenced by the surface roughness σ_S:

$$K_{adh} = \left(\frac{1}{a_1 \sigma_s^{\frac{1}{2}} + a_2} + a_3 + a_4 \sigma_s^{\frac{1}{2}} \right)^5 , \tag{32}$$

where a_1, a_2, a_3, a_4 are constants associated with the surface conditions.

The surface roughness is influenced by both the two failure mechanisms, according to equation (33) below [46]. In (33), x_{total} is the total wear depth and b_1, b_2 are two constants associated with the surface conditions.

$$\frac{d\sigma_s}{dt} = b_1 \left(\sigma_s + b_2 \right) \frac{dx_{total}}{dt} . \tag{33}$$

Equations (32) and (33) describe the root cause of the coupling. In order to develop a failure behavior model to describe the coupling, we make some simplifications to (32) and (33). From (32) and (33), we can see that K_{adh} is a function of σ_S and σ_S is a function of x_{total}. Thus, K_{adh} is a function of x_{total}. Since k_1 is determined by K_{adh} via (2), k_1 is also a function of x_{total}:

$$k_1 = g\left(x_{total} \right). \tag{34}$$

By using first order Taylor expansion as an approximation, and assuming that $g(0) = 0$, equation (34) becomes

$$k_1 = -k_1^{'} x_{total} . \tag{35}$$

Substituting (35) into (31) and solving for x_{total}, we have,

$$x(t) = \frac{k_2 - \exp\left\{ -k_1^{'} t + \ln k_2 \right\}}{k_1^{'}} . \tag{36}$$

In (36), $x(t)$ is the time-variant total wear depth and $k_1^{'}, k_2$ should be determined by conducting wear tests. Equation (36) describes the dependent failure behavior of the spool under the joint contribution of the adhesive and abrasive wear.

4.3. Experimental validation and discussions

In order to validate the developed model, a wear test is designed and implemented. Wear depths are monitored at fixed intervals by measuring the loss of weight due to the wear. The test setup is shown in Figure 9.

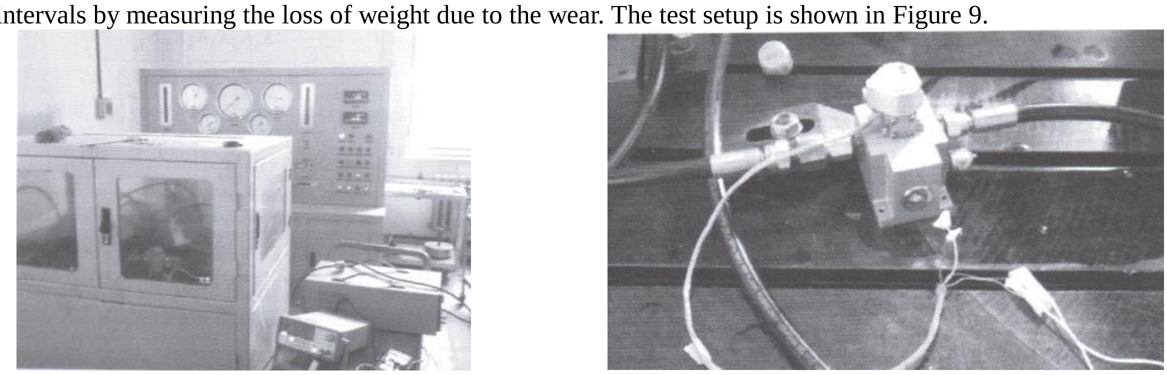

(a) Test equipment **(b) Specimen**

Figure 9 Test setups

The result of the wear test is shown in Figure 10 (the *x* and *y* axes are scaled, for confidential reasons). It should be noted that in the test, the quantity directly measured at each inspection is the mass-loss of the test specimen, denoted by Δm. The wear depth d in Figure 10 is calculated from Δm using the density of the valve material ρ and the nominal surface area A:

$$d = \frac{\Delta m}{\rho \cdot A} .$$

The model in (36) is fitted to the test data using the least square method. The result is shown as the solid line in

Figure 10.

As a comparison, we also develop a failure behavior model using the PoF method. In the PoF method, the two failure mechanisms are assumed to be independent. Since both PoF models suggest that the wear depth is a linear function of time (see (2) and (30)), the resulting failure behavior model is also a linear function of time,

$$x(t) = a + bt. \tag{37}$$

In (37), a and b are constants associated with the wear process and need to be estimated from test data. We also use the least square method to estimate the values of the parameters a and b. The result is represented by the dashed line in Figure 10.

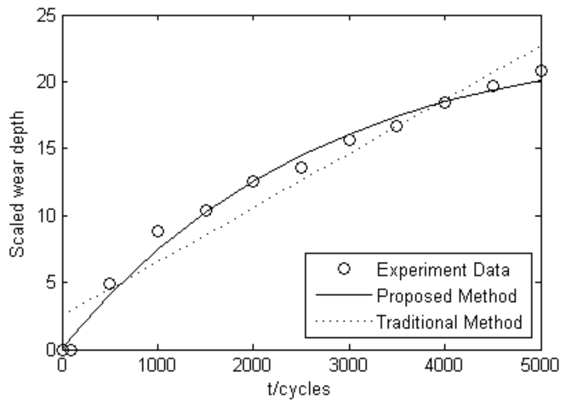

Figure 10 Experimental results and model fitting

It can be seen from Figure 10 that the compositional method provides a better fit to the test data than the linear model suggested by the PoF method. This conclusion is also justified by calculating the mean square error (MSE) for both models. The MSE of the model from the compositional method is 0.5298, which is far less than the 5.7981 of the one from the traditional method.

The differences can be explained by analyzing the trend of the test data. From the test data in Figure 10, we can see that the wear rates are decreasing over time, which suggests that the spool is in the running-wear period [46, 47]. In this period, the interaction between the two wear mechanisms tends to slow down the wear process [46, 47]. The PoF method ignores the interaction by assuming that the two failure mechanisms are independent. Therefore, inaccurate results are obtained. In the compositional method, on the contrary, the interaction is considered. Thus, it fits the experimental data better.

In existing dependency modeling methods, such as the multivariate distribution methods [9] and the copula-based methods [21], the dependent failure behavior is described by the joint distribution of the TTFs. The compositional method provides a PoF-based approach to determine the joint distribution. For example, by propagating the parametric uncertainties in (36) (see Table 1) using Monte-Carlo sampling, the joint TTF distribution of the spool is obtained. The result is given in Figure 11, where T_1 and T_2 represent the TTF predicted based on the abrasive wear model and adhesive wear model, respectively. The joint distribution $P\left(T_1 > t, T_2 > t\right)$ in Figure 11 represents the reliability of the spool at t, under the joint effect of the two failure mechanisms. Note that we assume the failure threshold of (36) is $p_{th} = 20$.

Table 1 Parametric uncertainties in (36)

Parameter	Distribution	Parameter	Distribution
$k_1^{'}$	$N\left(4\times10^{-4}, 7.58\times10^{-6}\right)$	k_2	$N\left(9\times10^{-3}, 1.80\times10^{-4}\right)$

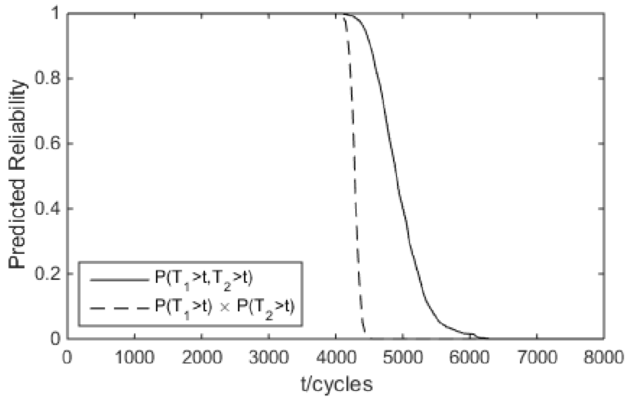

Figure 11 Reliability of the spool (i.e. predicted joint distribution of the TTFs)

In Figure 11, we also compare the $P(T_1 > t, T_2 > t)$ to the predicted reliability under the independence assumption, which is simply given by the product $P(T_1 > t) \times P(T_2 > t)$. It can be seen from Figure 11 that $P(T_1 > t, T_2 > t) \geq P(T_1 > t) \times P(T_2 > t), \forall t \geq 0.$ According to the definition by Lai and Lin [9], $P(T_1 > t, T_2 > t)$ is more diagonal-dependent than $P(T_1 > t) \times P(T_2 > t)$, which indicates that, the dependency among the two failure mechanisms increases the reliability of the spool. This is because, as discussed earlier, the spool is in the running-wear period, in which the wear processes are slowed down by the interactions among wear mechanisms [46, 47].

5. Conclusions

In this paper, a compositional method to model dependent failure behaviors is developed. The interactions among failure mechanisms are modeled as a combination of the three basic relations, competition, superposition and coupling. The method has the merit that it models physically the root cause of the dependency, so that a deterministic model can be derived to describe the dependent failure behaviors. The developed method is applied to model the failure behavior of a spool subject to two dependent failure mechanisms. A wear test has been implemented to validate the failure behavior model. The results demonstrate that the developed method is capable of modeling dependent failure behaviors.

In the work, we have considered dependency among failure mechanisms using a physics-based method. In the future, dependency among components can also be investigated in a similar way. For example, physics-based models can be developed to model the dependency due to shared loads, where the common loads shared by a group of components result in the dependency among them. Also, the dependency among components resulting from cascading failures can be considered, where the failure of some components increases the failure probability of other components.

Acknowledgement

This work has been performed within the initiative of the Center for Resilience and Safety of Critical Infrastructures (CRESCI, http://cresci.cn). The participation of Dr. Zhiguo Zeng to this research is partially supported by the National Natural Science Foundation of China (71671009). The research of Prof. Rui Kang is supported by the National Natural Science Foundation of China (61573043). The research of Prof. Yunxia Chen is supported by the National Natural Science Foundation of China (51675025). The authors would like to thank Mr. Xun Liao from Beihang university for his generous help in designing and conducting the wear test, and the editor and two anonymous referees for their helps in improving the quality of this paper.

References

[1]. Pecht, M. and A. Dasgupta. Physics-Of-Failure: An Approach to Reliable Product Development. in Integrated Reliability Workshop. 1995. Lake Tahoe, US: IEEE.
[2]. Tinga, T., ed. Principles of Loads and Failure: Applications in Maintenance, Reliability and Design. 2013, Springer: London.
[3]. McPherson, J.W., Reliability Physics and Engineering :Time-To-Failure Modeling. 2013, New York: Springer.
[4]. Collins, J.A., H.R. Busby and G.H. Staab, Mechanical Design of Machine Elements and Machines. 2009: Wiley: Newyork.
[5]. Zeng, Z., Kang, R., & Chen, Y. (2016). Using PoF models to predict system reliability considering failure collaboration. Chinese Journal of Aeronautics, 29(5), 1294-1301.
[6]. Malka, R., S. Nešić and D.A. Gulino, Erosion-Corrosion and Synergistic Effects in Disturbed Liquid-Particle Flow. Wear, 2007. 262(7): p. 791-799.
[7]. Zhu, S., H. Huang, L. He, Y. Liu, and Z. Wang, A Generalized Energy-Based Fatigue-Creep Damage Parameter for Life Prediction of Turbine Disk Alloys. Engineering Fracture Mechanics, 2012 (90): p. 89-100.
[8]. Kotz, S., C.D. Lai and M. Xie, On the Effect of Redundancy for Systems with Dependent Components. IIE Transactions, 2003. 35(12): p. 1103-1110.
[9]. Lai, C. and G.D. Lin, Mean Time to Failure of Systems with Dependent Components. Applied Mathematics and Computation, 2014. 246(0): p. 103-111.
[10]. Wang, Y. and H. Pham, Modeling the Dependent Competing Risks with Multiple Degradation Processes and Random Shock Using Time-Varying Copulas. IEEE Transactions On Reliability, 2012. 61(1): p. 13-22.
[11]. Feng, Q. and D.W. Coit, Reliability Analysis for Multiple Dependent Failure Processes: An MEMS Application. International Journal of Performability Engineering, 2010. 6(1): p. 100-108.
[12]. Peng, H., Q. Feng and D.W. Coit, Reliability and Maintenance Modeling for Systems Subject to Multiple Dependent Competing Failure Processes. IIE Transactions, 2011. 43(1): p. 12-22.
[13]. Feizjavadian, S.H. and R. Hashemi, Analysis of Dependent Competing Risks in the Presence of Progressive Hybrid Censoring Using Marshall–Olkin Bivariate Weibull Distribution. Computational Statistics & Data Analysis, 2015. 82(0): p. 19-34.
[14]. Xie, M. and C.D. Lai, Stochastic Ageing and Dependence for Reliability. 2006: Springer: London.
[15]. Murthy, D.P., M. Xie and R. Jiang, Weibull Models. Vol. 505. 2004: John Wiley & Sons: London.
[16]. Navarro, J. and T. Rychlik, Comparisons and Bounds for Expected Lifetimes of Reliability Systems. European Journal of Operational Research, 2010. 207(1): p. 309-317.
[17]. Navarro, J. and C. Lai, Ordering Properties of Systems with Two Dependent Components. Communications in Statistics—Theory and Methods, 2007. 36(3): p. 645-655.
[18]. Navarro, J., J.M. Ruiz and C.J. Sandoval, Properties of Coherent Systems with Dependent Components. Communications in Statistics - Theory and Methods, 2007. 36(1): p. 175-191.
[19]. Cui, L. and H. Li, Analytical Method for Reliability and MTTF Assessment of Coherent Systems with Dependent Components. Reliability Engineering & System Safety, 2007. 92(3): p. 300-307.
[20]. Nelsen, R.B., An Introduction to Copulas. 2007: Springer: Newyork.
[21]. Bunea, C. and T. Bedford, The Effect of Model Uncertainty On Maintenance Optimization. IEEE Transactions On Reliability, 2002. 51(4): p. 486-493.
[22]. Tang, X., D. Li, C. Zhou, and L. Zhang, Bivariate Distribution Models Using Copulas for Reliability Analysis. Proceedings of the Institution of Mechanical Engineers, Part O: Journal of Risk and Reliability, 2013. 227(5): p. 499-512.
[23]. Tang, X., D. Li, C. Zhou, K. Phoon, and L. Zhang, Impact of Copulas for Modeling Bivariate Distributions On System Reliability. Structural Safety, 2013. 44: p. 80-90.
[24]. Yang, Q., N. Zhang and Y. Hong, Reliability Analysis of Repairable Systems with Dependent Component Failures Under Partially Perfect Repair. IEEE Transactions On Reliability, 2013. 62(2): p. 490-498.
[25]. Hong, H.P., W. Zhou, S. Zhang, and W. Ye, Optimal Condition-Based Maintenance Decisions for Systems with Dependent Stochastic Degradation of Components. Reliability Engineering and System Safety, 2014. 121: p. 276-288.
[26]. Wang, S., X. Zhang and L. Liu, Multiple Stochastic Correlations Modeling for Microgrid Reliability and Economic Evaluation Using Pair-Copula Function. International Journal of Electrical Power & Energy Systems, 2016. 76: p. 44-52.
[27]. Botev, Z.I., P. L'Ecuyer, R. Simard, and B. Tuffin, Static Network Reliability Estimation Under the

Marshall-Olkin Copula. ACM Transactions on Modeling and Computer Simulation (TOMACS), 2016. 26(2): p. 14.

[28]. Jeddi, H. and M. Doostparast, Optimal Redundancy Allocation Problems in Engineering Systems with Dependent Component Lifetimes. Applied Stochastic Models in Business and Industry, 2015. 32(2) p. 199-208.

[29]. Zhang, X.P., J.Z. Shang, X. Chen, C.H. Zhang, and Y.S. Wang, Statistical Inference of Accelerated Life Testing with Dependent Competing Failures Based On Copula Theory. IEEE Transactions On Reliability, 2014. 63(3): p. 764-780.

[30]. Wu, S., Construction of Asymmetric Copulas and its Application in Two-Dimensional Reliability Modelling. European Journal of Operational Research, 2014. 238(2): p. 476-485.

[31]. Ebrahimi, N. and L. Hua, Assessing the Reliability of a Nanocomponent by Using Copulas. IIE Transactions, 2014. 46(11): p. 1196-1208.

[32]. Wang, Y. and H. Pham, A Multi-Objective Optimization of Imperfect Preventive Maintenance Policy for Dependent Competing Risk Systems with Hidden Failure. IEEE Transactions On Reliability, 2011. 60(4): p. 770-781.

[33]. Keedy, E. and Q. Feng, Reliability Analysis and Customized Preventive Maintenance Policies for Stents with Stochastic Dependent Competing Risk Processes. IEEE Transactions On Reliability, 2013. 62(4): p. 887-897.

[34]. Song, S., D.W. Coit, Q. Feng, and H. Peng, Reliability Analysis for Multi-Component Systems Subject to Multiple Dependent Competing Failure Processes. IEEE Transactions On Reliability, 2014. 63(1): p. 331-345.

[35]. Song, S., D.W. Coit and Q. Feng, Reliability for Systems of Degrading Components with Distinct Component Shock Sets. Reliability Engineering & System Safety, 2014. 132(0): p. 115-124.

[36]. Jiang, L., Q. Feng and D.W. Coit, Reliability and Maintenance Modeling for Dependent Competing Failure Processes with Shifting Failure Thresholds. IEEE Transactions on Reliability, 2012. 61(4): p. 932-948.

[37]. Rafiee, K., Q. Feng and D.W. Coit, Reliability Modeling for Dependent Competing Failure Processes with Changing Degradation Rate. IIE Transactions (Institute of Industrial Engineers), 2014. 46(5): p. 483-496.

[38]. Fan, M., Zeng, Z., Zio, E., Kang, R., & Chen, Y. (2017). A stochastic hybrid systems based framework for modeling dependent failure processes. PloS one, 12(2), e0172680.

[39]. Zhang, Q., Zeng, Z., Zio, E., & Kang, R. (2016). Probability box as a tool to model and control the effect of epistemic uncertainty in multiple dependent competing failure processes. Applied Soft Computing (available online) doi: 10.1016/j.asoc.2016.06.016.

[40]. Association, J.S.S.T. and V.A. Arlington, Failure Mechanisms and Models for Semiconductor Devices. JEDEC publication JEP122C, 2006.

[41]. Chatterjee, K., M. Modarres and J. Bernstein, Fifty Years of Physics of Failure. Journal of Reliability Information Analysis Center, 2012. 20(1): p. 1-5.

[42]. Archard, J.F., Contact and Rubbing of Flat Surfaces. Journal of Applied Physics, 1953. 24(8): p. 981-988.

[43]. Whiteside, M.B., S.T. Pinho and P. Robinson, Stochastic Failure Modelling of Unidirectional Composite Ply Failure. Reliability Engineering & System Safety, 2012. 108: p. 1-9.

[44]. Chookah, M., M. Nuhi and M. Modarres, A Probabilistic Physics-Of-Failure Model for Prognostic Health Management of Structures Subject to Pitting and Corrosion-Fatigue. Reliability Engineering and System Safety, 2011. 96(12): p. 1601-1610.

[45]. Plumbridge, W.J. and R.J. Matela, Structural Integrity and Reliability in Electronics. 2004: Springer: London.

[46]. Chen Y., Gong W., and Kang R. Coupling behavior between adhesive and abrasive wear mechanism of aero-hydraulic spool valves. Chinese Journal of Aeronautics 29, no. 4 (2016): 1119-1131.

[47]. Engel, P.A., Failure Models for Mechanical Wear Modes and Mechanisms. IEEE Transactions On Reliability, 1993. 42(2): p. 262-267.